Synergistic Interaction between Anionic and Nonionic Surfactant: Application of the Mixed Micelles Templates for the Synthesis of Silver Nanoparticles

Naved Azum[1,2,], Khalid A. Alamry[1,2], Sher Bahadar Khan[1,2], Malik Abdul Rub[1,2], Abdullah M. Asiri[1,2] and Yasir Anwar[3]*

[1]Center of Excellence for Advanced Materials Research, King Abdulaziz University, P.O. Box 80203, Jeddah, Saudi Arabia 21589
[2]Chemistry Department, Faculty of Science, King Abdulaziz University, P.O. Box 80203, Jeddah, Saudi Arabia 21589
[3]Department of Biology, Faculty of Science, King Abdulaziz University, P. O. Box. 80203, Jeddah, 21589, Saudi Arabia
[*]E-mail: navedazum@gmail.com

Interaction between the anionic and nonionic surfactant at bulk and air/water interface has been studied. The synergistic interaction between surfactants was found in both in bulk solution as well as the interface. The different physicochemical parameters of the free surfactant monomers up to the point of their critical micelle concentration (*cmc*) have been evaluated and discussed in detail. The synergistic interactions have been analyzed using various theoretical models reported i.e., Clint, Rubingh, Maeda and Rosen models. The spectrophotometric and structural analyses have been achieved for the formation of silver nanoparticles using sodium borohydride as reducing agents and pure as well as mixed surfactant systems as capping agents. Antimicrobial activities of the synthesized nanoparticles were performed against both Gram-negative (*P. aeruginosa and Klebsiella Pneumonia*) and Gram-positive (*Micrococcus luteus*) bacteria.

1. INTRODUCTION

Surfactants have a unique position among the chemical compounds. They have a wide spectrum of applications including environmental, medical, petroleum. These surfactants are also may be used in the laundry products, production and processing of food, health and personal care products, crop protection and petroleum [1-3]. The main reasons of the omnipresent placement of surfactant are

due to its ability to alter the properties of surfaces or interfaces. The scientific interest in increasing the performance of these systems led to the research into surfactant mixture (mixed surfactant systems). The surfactants mixture has gained importance in the scientific fields due to their (i) better performance (ii) cost effectiveness (iii) enhanced the adsorption of various drugs (iv) improve the tolerance of water hardness etc [4-7]. The better performance of mixed systems over the single surfactant is due to the synergism observed between two or more components. The synergism can be understood by the taking the example of cosmetic industry, where surfactants are used in low concentration to stay away from skin irritation. The binary and ternary mixtures of surfactants have often been studied by surface tension, fluorescence, electric conductivity, NMR, turbidity and solubilization etc to investigate micellar compositions, aggregation number, molecular interactions parameters, phase separation and thermodynamics parameters [8-21].

Mixed micelles framed by two or more surfactants combinations such as cationic/cationic, cationic/anionic, cationic/nonionic have been studied in detail by several workers. Numerous theoretical models have been proposed for interpretations of the mixed systems to calculate the interaction parameters at air/water interface or in micellar phase. The Clint's model [22] relates the critical micelle concentration (cmc) with mole fraction of components by using the phase separation model. The simplest and used theoretical model is Rubingh's model [23] that relates the monomer concentration to micellar concentration. This Rubingh's model has been mostly used for treatment of a nonideal mixing even after the development of more complex models. Motomura and Aratono [24] build up a model specifically an effort of overcoming the shortcomings of Rubingh's model. Maeda [25] has presented a theoretical analysis of ionic-nonionic mixed micelles, which involves two parameters. The model, based on a thermodynamic point of view, is valid for a solution with moderately high ionic strength.

In recent years, nanotechnology has persuaded great research advancement in the various fields of science. The study of small particles (1-100 nm) which can be used in various fields: i.e., chemistry, biology, physics, material science and engineering [26-29]. Since surfactants have emerged as stabilizing agents for the synthesis of nanoparticles. They have unique properties because of its nano size. Colloidal silver nanoparticles have distinct properties such as chemical stability, good conductivity, antibacterial, catalytic activity [30-34]. These particles have a specific position in the field of bio labeling, sensor, electronics and other medical application such as drug delivery and disease diagnosis. However, nanoparticles tend to be unstable in solution so special precaution safeguard is needed to avoid aggregation and oxidation during the synthesis of colloidal nanoparticles in solution. Surfactants such as cetyttrimethylammonium bromide (CTAB), were used as a modifier. These compounds control the particle size distribution, shape, and further oxidation. A lot of literature is available for use of single surfactant in the preparation of silver nanoparticles. However, the best of our knowledge till now there is a limited report in the literature, where a mixed system of surfactants has been investigated.

Take into account the significance of mixed systems, it would be very appealing to know the physico-chemical properties of mixed system and whether there is any influence of mixed system on size, shape, stability and other properties of silver nanoparticles. A relative study of single surfactants and mixed surfactants can provide better imminent into the silver nanoparticles stability and properties.

2. EXPERIMENTAL

2.1 Materials

The chemicals SDS (Sigma, 99%), Brij-58 (Sigma, 98%), AgNO$_3$ (Koch-light Laboratories, 99%), NaBH$_4$ (BDH) were used as received. Appropriate amount of solutes were dissolved in de-ionized double distilled water (DDW) (having specific conductivity in the range 1–3 μScm^{-1}) to make stock solutions. For fluorimetric experiments the solutions were prepared with DDW having the pyrene (Sigma, 98%) as a probe (1μM). *Pseudomonas aeruginosa, Klebsiella Pneumonia and Micrococcus luteus* were provided by Biology Lab King Abdulaziz University. Nutrient Agar and Luria–Bertani (LB) medium used in growing and maintaining the bacterial cultures were supplied by HiMedia Laboratories.

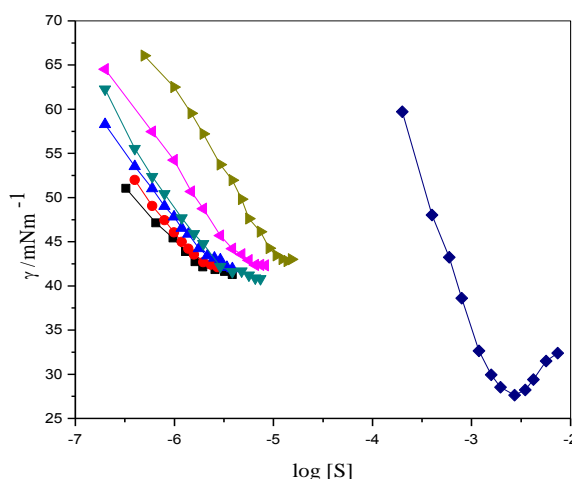### 2.2 Measurements

2.2.1 Surface tension measurements

Figure 1. Plots of surface tension vs. log [S] (total amphiphile molar concentration) for SDS+Brij-58 mixture in at 298.15 K: $\alpha_{SDS} = 0$, ■; $\alpha_{SDS} = 0.1$, ●; $\alpha_{SDS} = 0.3$, ▲; $\alpha_{SDS} = 0.5$, ▼; $\alpha_{SDS} = 0.7$, ◀; $\alpha_{SDS} = 0.9$, ▶; $\alpha_{SDS} = 1.0$, ♦.

The ring detachment method has been applied to determine the surface tension using attension tensiometer (Sigma 701) at 298.15 ± 0.2K. The Du Nouy principle is obeyed by attension tensiometer. According to the Du Nouy principle the force to lift the ring from the surface of a liquid is related to the surface tension of that liquid by the relation:

$$F = 2\pi \, (r_1 + r_2) \, \gamma \qquad (1)$$

Where r_1, and r_2, are the radius of inner ring and outer ring of the liquid film respectively. The ring was heated in alcohol flame before performing a new experiment. The Fig. 1 shows a plot between measured surface tension values vs. logarithm of amphiphile concentration. The accuracy of the measurements was within ± 0.1 mN m^{-1}.

2.2.2 Fluorescence measurements

The steady-state fluorescence measurements were achieved using Hitachi F-7500 flourometer using a quartz cuvette of 1 cm path length. Pyrene was used as a probe. The excitation wavelength of 335 nm was used and the emission spectra were recorded in the wavelength range of 350–450 nm. Both emission and excitation slit width were fixed at 2.5 nm. For determination of aggregation number, N_{agg}, the steady state fluorescence quenching measurements were performed using cetylpyridinium chloride (CPC) as a quencher.

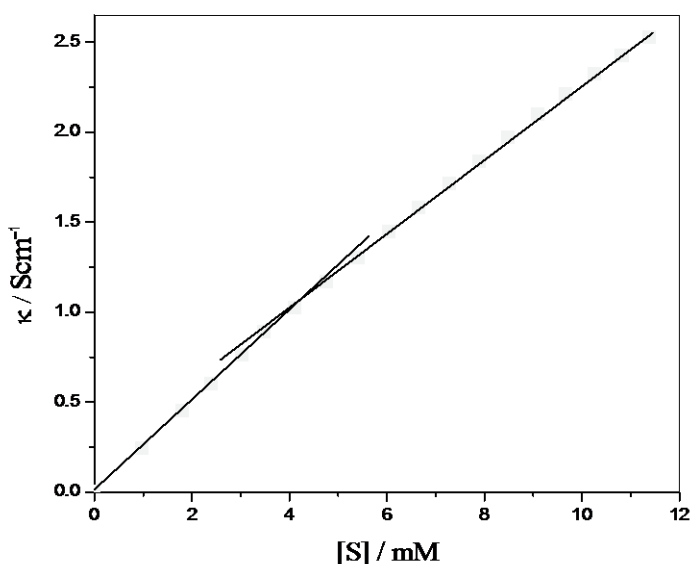## 2.2.3 Conductometric measurements

Figure 2. Plot of specific conductivity vs. concentration of SDS.

Equip-tronics conductivity meter, model EQ661, and a dip cell having cell constant 1 cm^{-1} were employed to performed the conductivity measurements at 298.15 ± 0.2K. The conductivity was measured by successive addition of concentrated stock solution in water. A break in the conductivity vs surfactant concentration curve signals onset of micellization process as shown in Fig. 2. Conductometry is considered to be a basic structure-sensitive method for investigating micellar systems. This approach is completely based on the concepts that were developed in physical chemistry when studying the conductivity of electrolytes. Conductivity can be defined as the ability of a solute to pass current through the ions. The specific conductivity (κ) = conductance (G) x cell constant (K).

2.2.4 Characterization of silver sol

The absorption spectra of prepared silver sols were recorded on a UV-vis spectrometer (evolution 300 UV-Vis spectrophotometer). The SEM imagings of silver nanostructures were performed on JEOL scanning electron microscope (JSM-7600, Japan).

2.2.5 Disc diffusion method for antibacterial activity

The synthesized nanoparticle's antimicrobial activities were performed against both Gram-negative (*P. Aeruginosa and Klebsiella Pneumonia*) and Gram-positive (*Micrococcus luteus*) bacteria. The bacterial inoculums was uniformly spread using a sterile cotton swab on a sterile Petri dish containing Nutrient Agar. Three different concentrations of nanoparticle (A, B and C) were used to check its antibacterial activity. For this the discs was dipped in different concentrations of nanoparticles and then transfer to a Petri plate containing a bacterial culture. Then, under aerobic conditions, these plates were incubated for 24 h at 36ºC ± 1ºC and confluent bacterial growth was observed after incubation. Inhibition of the bacterial growth was measured in mm.

3. RESULTS

3.1 Critical micelle concentration of pure and mixed surfactant systems

The surfactants when present at low concentration behave like a simple electrolyte and exist as free monomers. However, at a concentration where monomers form aggregate known as critical micelle concentration (*cmc*). The *cmc* values of pure SDS were evaluated from the conductometry and tensiometry techniques. While the cmc values for pure BRIJ-58 and its mixed systems with SDS evaluated by only tensiometry technique.

Table 1. Different physico-chemical parameters for SDS/Brij-58 mixture

α_{SDS}	$10^5\ cmc_{exp}$ (M)	$10^5\ cmc_{ideal}$ (M)	X_1	X_1^{ideal}	β^m	f_1	f_2	B_0	B_1
0.0	0.182								
0.1	0.189	0.202	0.049	0.00006	-7.429	0.0012	0.9821	-17.233	0.033
0.3	0.212	0.259	0.108	0.00025	-7.904	0.0018	0.9119	-17.233	0.441
0.5	0.290	0.363	0.120	0.00057	-7.192	0.0038	0.9016	-17.233	0.270
0.7	0.470	0.605	0.135	0.00134	-6.506	0.0076	0.8881	-17.233	0.956
0.9	0.986	1.810	0.223	0.00514	-7.250	0.0125	0.6972	-17.233	0.211
1.0	317								

Figure 1 shows surface tension trends and show surface tension curves of total surfactant concentration vs. surface tension. Surface tension of the solvent (water) was 70 or 71, which reduces as the surfactant solution introduced (Fig. 1) until the *cmc*. The *cmc* value of Brij-58 obtained was much lower than SDS. For Brij-58, micellization is chiefly due to hydrophobic interaction amid hydrocarbon chains. The hydrophobic group simply alienated from the aqueous phase, whereas for ionic surfactants, high concentration required to conquer the electrostatic repulsion between ionic head groups during the

micellization. Like the single surfactants mixed surfactants are also aggregated and form micelles but the tendency to aggregate are different from that of single ones. In binary mixtures, cmc values increases with increase in mole fraction of SDS (Table 1). The results indicate that the added Brij-58 assist SDS in the early micelle formation.

Figure 2 shows increase of conductivity as the concentration of SDS increases until an inflection point (concentration at which monomers start to aggregate). Above this point conductivity still increases with concentration but with a decrease in gradient. Below cmc, ionic surfactants behave as strong electrolytes and dissociate completely into its ions according. At and above the cmc, the mobility of ions slows down. Above cmc, mobility of ions decreases because micelles are partially ionized. The cmc value of SDS was found to be 4.48 mM and found to be in good agreements with the cmc value evaluated by tensiometric method (3.17 mM).

3.2 Interaction of SDS with Brij 58 surfactants in mixed micelles

When the two or more surfactants mixed together to form a mixed micelle the combination can be either ideal or non-ideal. The Clint's model which is based on pseudophase thermodynamic model can be employ to examine the ideality of the mixed micelles [22]. The Clint's model is a very simple theory, show that the pure components are non-interacting and their individual cmc_s be a sign of their relative tendency toward mixed micellization. The ideal cmc (cmc_{ideal}) can be calculated by the equation;

$$\frac{1}{cmc_{ideal}} = \sum_{i}^{n}\left(\frac{\alpha_i}{cmc_i}\right) \qquad (1)$$

For two components mixed system

$$\frac{1}{cmc_{ideal}} = \frac{\alpha_1}{cmc_1} + \frac{\alpha_2}{cmc_2} \qquad (2)$$

where cmc_1 and cmc_2 are the critical micelle concentrations of SDS and Brij-58 respectively. Any deviation from cmc_{ideal} would, however, account for interactions among surfactants. Divergence in +ve and −ve sides suggests antagonism and synergism respectively. In our systems, the cmc values are come out to be lower than cmc_{ideal} values [Table 1], suggesting synergism, also indicate non-ideal behavior of mixing. It is confirmed from Table 1 that the cmc values are lower than that of pure SDS and increases gradually with increasing mole fraction of the SDS in solution. This indicates that the hydrophobic effects are dominates in the formation of mixed micelle. The charged head groups of SDS are coiled around by the chains of ethoxylate of Brij-58 molecules, screening the electrostatic repulsions and favoring micelle formation resulting in decrease in cmc. The micellar mole fraction at cmc (X_1) in mixed systems as a function of component 1(SDS), has been evaluated in the light of Rubingh's equation [23]:

$$\frac{[X_1^2 \ln(cmc_{exp}\alpha_1 / cmc_1 X_1)]}{(1 - X_1)^2 \ln[cmc_{exp}(1 - \alpha_1) / cmc_2 (1 - X_1)]} = 1 \qquad (3)$$

where cmc_1, cmc_2 and cmc_{exp} denote the cmc values of the amphiphiles 1, 2 and mixed system respectively. The ideal mole fraction (X_1^{ideal}) of SDS can be calculated to equation (4):

$$X_1^{\text{ideal}} = \frac{\alpha_1 cmc_2}{\alpha_1 cmc_2 + \alpha_2 cmc_1} \qquad (4)$$

Table 1 state that X_1^{ideal} is lower than that of X_1. This suggests a higher contribution of the SDS component to the mixed micelles than the ideal one and positive interaction in the mixed micellar phase. The interaction parameter, β^{m}, of mixed micelle formation given by

$$\beta^{\text{m}} = [\ln(cmc_{\text{exp}}\,\alpha_1 / cmc_1 X_1)]/(1 - X_1)^2 \qquad (5)$$

The β^{m} is a scale not only for the degree of interaction, but also reports for the deviation from ideality between the two amphiphiles. The attractive interaction results from $-$ve β^{m} values, the more $-$ve its value, the larger the interaction. The Table 1 contains the values obtained for the current binary surfactant system. The β^{m} values are not constant and $-$ve throughout, suggest the strong synergism in the system. The activity coefficients of the surfactants within the micelle can be relates with β^{m}:

$$f_1 = exp\left[\beta^{\text{m}}(1 - X_1)^2\right] \qquad (6)$$
$$f_2 = exp\left[\beta^{\text{m}}(X_1)^2\right] \qquad (7)$$

The activity coefficients are also shown in Table 1. It is clear from the table that values of micellar mole fraction of SDS (X_1) are small, which suggest that SDS in mixed micelle is remote from its standard state. The f_2 values are closer to unity, which represents that Brij-58 in the mixed micelle is near to its standard state.

For ionic/non-ionic surfactants mixed systems of moderately high ionic strength (negligible short range electric interaction) Maeda model can be applied [25]. The major difference between Rubingh and Maeda is electric interaction. In Rubingh model long-range electrical interaction exists in mixed micelles. According to Maeda "in the micellar phase, the presence of non-ionic surfactant molecules in ionic/non-ionic mixed system, decreases the repulsion between ionic head group". The anticipated equation for free-energy change due to the micellization process is

$$\Delta G_{Maeda}^o = RT(B_o + B_1 X_1 + B_2 X_1^2) \qquad (8)$$

Where

$$B_o = lnX_{cmc,2} \qquad (9)$$

$X_{\text{cmc},2}$ is the *cmc* of Brij-58 in mole fraction scale, and B_2 is the interaction parameter in the micellar phase ($B_2 = -\beta^{\text{m}}$). And B_1 can be calculated by using the equation

$$B_1 + B_2 = \ln\left(\frac{X_{cmc,1}}{X_{cmc,2}}\right) \qquad (10)$$

The calculated results of all parameters are given in Table 1. The B_1 values being positive clearly indicate that there is no chain-chain interaction between SDS and Brij-58.

3.3 Surface properties of SDS/Brij-58 mixed system

The water has a high surface tension value because of strong hydrogen bonding between water molecules. When a surface active compound is added in it, the molecules of surfactant first remain populated at interface to avoid the interaction between hydrophobic part (tail) and water molecules and hydrophilic part (head group) are obscured in aqueous environment. In this way the hydrogen bonding present on the surface foil and surface tension start to decrease. The surface tension (γ) continues decreases until the air/water interface is flooded with surfactant monomers. The surface tension does

not change after reaching a certain concentration. This concentration is called as *cmc* and the constant value of surface tension (γ_{cmc}) at *cmc* is measure the efficacy of the surfactant to populate the air/water interface in the form of a monolayer prior to micellization. It can be also predicted from Gibbs surface excess (Γ_{max}) by using the following equation:

$$\Gamma_{max} = -\frac{1}{2.303nRT} \lim_{C \to cmc} \left(\frac{d\gamma}{d\log S}\right) \qquad (11)$$

Where n is equivalent to the number of species in solution and n is taken as unity for Brij-58, 2 for SDS and 3 for mixtures. R is the universal gas constant and T is temperature in absolute scale. Γ_{max} can be used to calculate minimum area per molecule by the relation:

$$A_{min} = 10^{18}/(N_A\Gamma_{max}) \qquad (12)$$

Γ_{max} is directly proportional to surface activity, the higher the value, the higher the surface activity. SDS is the most surface active (Table 2).

Table 2. Interfacial parameters for SDS/Brij-58 mixture

α_{SDS}	$10^5 C_{exp}$ (M)	$10^5 C_{ideal}$ (M)	X^{σ}_1	β^{σ}	$10^7\Gamma_{max}$ (mol m^{-2})	A_{min} (nm)	Π (mN m^{-1})
0.0	0.959				20.666	0.803	27.756
0.1	0.106	1.06	0.337	-16.728	8.204	2.023	27.653
0.3	0.140	1.36	0.356	-14.548	8.624	1.925	26.772
0.5	0.172	1.88	0.376	-13.797	8.930	1.859	28.546
0.7	0.308	3.06	0.391	-12.113	9.430	1.760	27.663
0.9	0.804	8.16	0.430	-10.391	11.377	1.459	27.392
1.0	49.200				29.246	0.567	38.267

Inspecting the data in Table 2 explains A_{min} values for mixtures are higher than that of pure surfactants. This confirms additional compactness of mixtures at the air/water interface, which could attribute to the orientation of the molecules at the interface. The value of A_{min} decreases with increasing the mole fraction of SDS. The hydrophobic interactions between the different hydrophobic tails are associated with the more compact adsorbed mixed monolayer at the air/water interface and the van der Waal's forces between the anionic and nonionic group.

The interfacial compositions (X^{σ}_1) and interaction parameters (β^{σ}) at the Langmuir monolayer for two different surfactants were evaluated using the Rosen's model [35]. The composition of the adsorbed monolayer (X^{σ}_1) formed by the two surfactants in the mixed system in the premicellar region can be evaluated by Rosen's model. The (X^{σ}_1) can be calculated iteratively by solving the equation:

$$\frac{[X^{\sigma^2}_1 \ln(C_{mix}\alpha_1 / C_1 X^{\sigma}_1)]}{(1 - X^{\sigma}_1)^2 \ln[C_{mix}(1 - \alpha_1)/C_2(1 - X^{\sigma}_1)]} = 1 \qquad (13)$$

where C_{mix}, C_1 and C_2 are the concentrations of the mixture, pure surfactant SDS and Brij-58, respectively, at a fixed γ value, α_1 is the stiochiometric mole fraction of surfactant (SDS) in the solution. The value was then used to evaluate the interaction parameter (β^{σ}) at the air/solution interface using

$$\beta^{\sigma} = [\ln(C_{\text{mix}}\, \alpha_1 / C_1 X^{\sigma}_1)]/(1 - X^{\sigma}_1)^2 \qquad (14)$$

The X^{σ}_1 and β^{σ} values of the mixture are presented in Table 2. The ideal monolayer has a value zero for amphiphile-amphiphile interaction parameter while negative and positive for synergistic and antagonistic interactions, respectively. Higher value of X^{σ}_1 compare to α_1 at lower mole fractions indicated more propensity of SDS to preferentially populate the interface as compared to the Brij-58.

3.4 Synergism

The extent of synergism between two or more surfactants depends on interaction between surfactants and appropriate properties of the surfactants in different phases. This phenomenon can be divided into two parts: (i) surface tension decline efficiency and (ii) surface tension effectiveness.

In the surface tension decline efficiency, two conditions exist: (a) β^{σ} should be negative and (b) $|\beta^{\sigma}|>|\ln(C^{\sigma}_1/C^{\sigma}_2)|$. Similarly, in mixed micellar phase $|\beta^{m}|>|\ln(cmc_1/cmc_2)|$. It is clear from Tables 1 and 2 that all these requirements are found, thereby the mixing of SDS+Brij-58 under study conditions exhibit synergistic behavior.

In the surface tension reduction effectiveness, where cmc_{mix} is lower than individual surfactant cmcs, The condition of synergism are: (a) $\beta^{\sigma} - \beta^{m}$ must be negative and $|\beta^{\sigma} - \beta^{m}|>|\ln(C^{\sigma}_1 cmc_2/cmc_1 C^{\sigma}_2)|$. The data in Tables 1 and 2 reveal that the mixed system under investigation synergism.

3.5 Thermodynamics of micellization and interfacial adsorption

The thermodynamic parameters such as Gibbs free energy change on ideal state (ΔG^m_{ideal}), free energy change (ΔG^m), enthalpy (ΔH^m), and entropy (ΔS^m) change in the process of micellization can be used to elucidate the deviation from ideal behavior and micellization process. On the basis of regular solution theory (RST), the thermodynamic parameters can be calculated by using the following equations

$$\Delta G^m_{ideal} = RT(X_1 ln X_1 + X_2 ln X_2) \qquad (15)$$
$$\Delta G^m = RT(X_1 ln f_1 X_1 + X_2 ln f_2 X_2) \qquad (16)$$
$$\Delta H^m = RT(X_1 ln f_1 + X_2 ln f_2) \qquad (17)$$
$$\Delta S^m = (\Delta H^M - \Delta G^M)/T \qquad (18)$$

The thermodynamic parameters of micellization are listed in Table 3. It is finds that the values ΔH^m ΔG^m and ΔG^m_{ideal} are negative, but ΔS^m are positive, implying the spontaneous process of micellization. It is clear from Table 3 that the Gibbs energy change of micellization is more negative than the ideal value, favoring the micelle formation of mixed systems. This situation can happen when a compact, mixed micelle forms.

The standard free energy of micellization per mole of monomer unit (Brij-58 and SDS/Brij-58) is given by the relation (considering the negligible degree of counter ion dissociation)

$$\Delta G^o_m = RT ln X_{cmc} \qquad (19)$$

Table 3. Thermodynamic parameters SDS/Brij-58 mixture

α_{SDS}	$-\Delta G^m$ (kj mol^{-1})	$-\Delta H^m$	ΔS^m	$-\Delta G^m_{ideal}$ (kj mol^{-1})	$-\Delta G_{add}$ (kj mol^{-1})	$-\Delta G_{min}$ (kj mol^{-1})	$-\Delta G_{exc}$ (kj mol^{-1})	$-\Delta G^o_{Maeda}$ (kj mol^{-1})	$-\Delta G^o_m$ (kj mol^{-1})
0.0				55.69	56.13	20.44			42.69
0.1	1245.57	861.04	1.29	61.14	76.31	51.61	0.86	42.66	42.60
0.3	2393.29	1886.65	1.70	60.46	73.36	50.12	1.88	42.60	42.32
0.5	2401.57	1881.71	1.74	59.95	73.51	46.41	1.88	42.37	41.54
0.7	2413.92	1882.37	1.78	58.51	69.68	44.89	1.88	42.09	40.34
0.9	3411.62	3112.75	1.00	56.13	62.58	37.45	3.11	41.69	38.51
1.0				45.94	37.29	10.85			24.21

This free energy is compared with that obtained using Maeda's model. From Table 3, the close resemblance of ΔG^o_{Maeda} and ΔG^o_m for SDS/Brij-58 system also reflects negligible counter ion dissociation. The standard free energy of micellization calculated by the equation (19) is translated into the standard free energy of adsorption at the air water interface using the equation [36, 37]

$$\Delta G^o_{ad} = \Delta G^o_m - \pi/\Gamma_{max} \qquad (20)$$

Where Π is surface pressure at *cmc*. The ΔG^o_{ad} values are all negative throughout (Table 3), reveals spontaneity of the adsorption at the air/water interface. The magnitude of ΔG^o_{ad} is more than the ΔG^o_m showing that the latter to be less spontaneous due to the hydrophobicity of amphiphiles, which lead them toward air/water interface. It is concluded that the adsorption is primary and spontaneous process compared to micelle formation which is a secondary and less spontaneous process.

The free energy of surface at equilibrium (G_{min}) points out the synergism in the mixed adsorbed monolayer [36] and can be calculated by the equation:

$$G_{min} = A_{min}\gamma_{cmc}N_A \qquad (21)$$

where, γ_{cmc}, A_{min} and N_A are the surface tension of the surfactant system at equilibrium, minimum surface area and Avogadro number respectively. It may be defined as the work needed to make a surface area per mole or free energy change accompanied by transition from the bulk phase to the surface phase of the solution. The more thermodynamically a stable surface is formed at lower level of free energy, which is a measure of evaluation of synergism. Since the obtained values are lower in magnitude (Table 3), it can be inferred that thermodynamically stable surfaces are formed with synergistic interaction.

The excess free energy of micellization, ΔG_{ex}

$$\Delta G_{ex} = [X_1 \ln f_1 + (1 - X_1)ln f_2]RT \qquad (22)$$

The negative values (Table 3) confirm the thermodynamic stability of mixed system compared to the micelle formed by the individual surfactants.

3.6 Micellar aggregation numbers and micropolarity

The steady state fluorescence quenching method is an appropriate method for determining the micellar aggregation numbers [38-40]. If a luminescent probe, pyrene, is added in a micellar solution having [M, unknown micelle concentration] and [Q, a quencher of concentration], then the measured ratio of intensities in the presence (*I*) and absence (*I*o) of quencher is related as [41]

$$\ln\left(\frac{I_0}{I}\right) = \frac{N_{agg}[Q]}{[S]_T - cmc} \qquad (23)$$

Equation (23) predicts a linear plot between $\ln(I_o/I)$ and [Q] with a slope equal to $N_{agg}/([S]_T)$-*cmc*, which gives the values of N_{agg}. Values of N_{agg} determined from plots of are reported in Table 4. It is clear from Table 4 that the N_{agg} increases with the mole fraction of SDS. This can be explained on the basis of polydisperse nature of SDS, which could produce well-defined micelles of higher N_{agg}. This result is in line with previous results that mixed micelle contain more SDS (higher value of X_1).

Table 4. Average aggregation numbers (N_{agg}), Stern-Volmer constant (K_{sv}), micropolarity and dielectric constant for the SDS/Brij-58 mixed system, evaluated on the basis of steady-state fluorescence quenching technique

α_{SDS}	N_{agg}	K_{sv}	I_1/I_3	D_{exp}	D_{ideal}
0.0	070	2.39	1.31	24.62	24.62
0.1	047	1.34	1.27	21.28	24.82
0.3	070	2.39	1.26	20.22	25.06
0.5	083	3.11	1.26	20.18	25.11
0.7	096	3.59	1.24	19.22	25.17
0.9	137	6.53	1.25	19.60	25.54
1.0	065	11.15	1.36	28.75	28.75

The aforementioned outcome can further be explained on the basis of quenching. The Stern-Volmer binding constant (K_{sv}), relates the strength of hydrophobic environment, can be evaluated by determining the first order quenching rate constant using the relation

$$\frac{I_0}{I} = 1 + K_{sv}[Q] \qquad (24)$$

The bimolecular quenching and unimolecular decay can be understood by the Stern-vomer constant (K_{sv}). The K_{sv} is the product of the rate constant of the quenching process and the lifetime of the probe in the absence of bimolecular quenching [42]. The greater the solubility of the probe and quencher, higher would be the K_{sv} value. High K_{sv} values (Table 4) suggest an increase in quenching due to the presence of both pyrene and quencher in the strong hydrophobic environment.

The micropolarity of a microevironment can be calculated by the ratio of the probe first and third peak. The micropolarity is directly related to the environment in which pyrene is solubilized and senses the degree of hydrophobocity of that environment. The I_1/I_3 values are also associated with a local polarity index of a solubilization site. The polar environment has higher value of I_1/I_3 while nonpolar has low value as in hydrocarbon solvent [43]. The value of I_1/I_3 as shown in Table 4 show alcohol like environment.

The experimental apparent dielectric constant (D_{exp}) of the medium can be calculated by using the following equation [44-48]

$$\frac{I_1}{I_3} = 1.000461 + 0.01253 D_{exp}$$

(25)

The D_{exp} values are given in Table 4. The data show no definite trend and values are close to the D_{exp} values for methanol and ethanol [49]. This also confirms that the solubilized pyrene is in a short alcohol-like environment.

According to Turro et al. [50], in an ideal system the dielectric constant inside the mixed micelle can be calculated as:

$$D_{ideal} = \sum X_i D_i$$

(26)

The D_{exp} and D_{ideal} values for current systems are given in Table 5. It is clear from these values that the $D_{exp} \neq D_{ideal}$, an expected result because of attractive interaction inside the micelle.
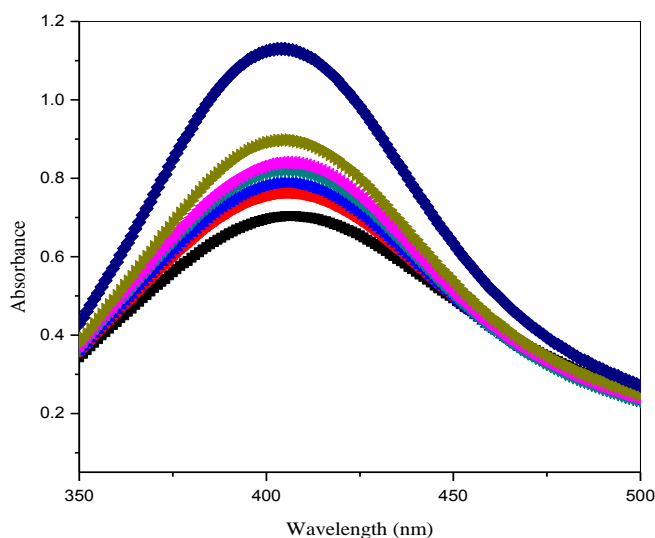
3.7 Characterization of AgNPs

Figure 3. UV-visible spectra of silver nanoparticles as a function of time (min): 0.0, ■; 15, ●; 30, ▲; 60, ▼; 90, ◄; 175, ►; 350, ♦.

In the synthesis of AgNPs, aqueous solution of $AgNO_3$ and pure (SDS, Brij-58) and mixed surfactants (SDS+Brij-58) were utilized as salt precursor and capping agent of AgNPs, respectively. The aqueous freshly prepared solution of $NaBH_4$ was added as a reducing agent. The colorless reaction mixture was transformed into yellow color after the addition of $NaBH_4$ which was due to growth of AgNPs. The growth of AgNPs was monitored by measuring the absorbance (spectrophotometrically) of the reaction product.

The synthesis and stabilization of nanoparticles (NP) can be controlled by surfactants; they can control the size and shape of NPs depending on their types and length. In our study, the AgNPs formation was confirmed from observing the color change (colorless to yellow) supporting the reduction of Ag (I) ions to Ag(0), and confirmed from the UV spectra. The Plasmon absorption band

of the AgNPS strongly depends on their size and shape. Spherical AgNPs show Plasmon band at ~ 410 nm (Fig 3) that becomes red shifted with increase in particle size. The morphology and size distributions from FESEM measurements are presented in Fig 4.
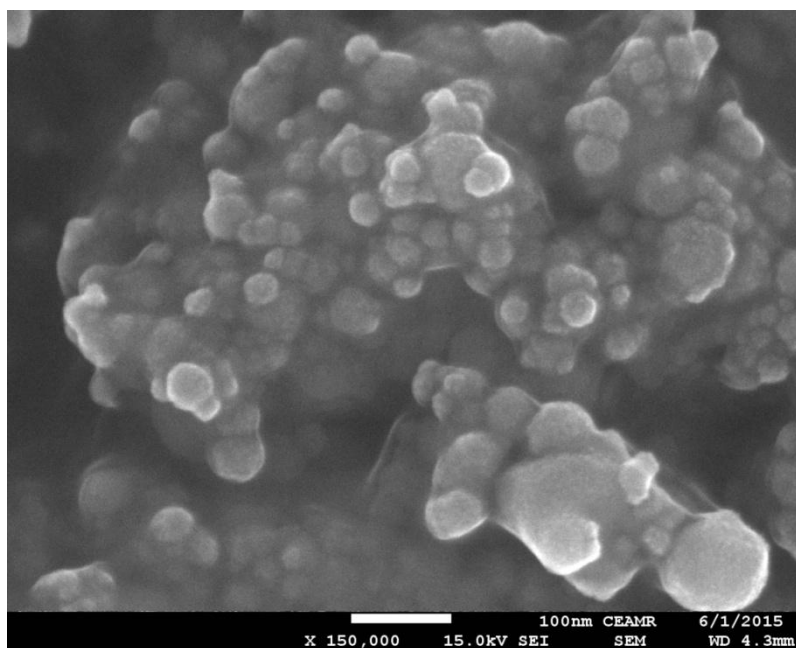

Figure 4. Typical FESEM images of AgNPs.

The particle shapes were spherical and the average size reported in Fig 4 show that the sizes in the pure micelle of were 50 nm. Synthesis of nanoparticles was considered prospective in the mixed micellar templates herein studied.

3.8 Antibacterial activity

The effects of AgNPs on the cell of bacteria are complicated [51]. However, a number of mechanisms have been studied on the action of AgNPs on the bacterial cell [52]. Some of these mechanisms were summarized and presented as follows: (i) the ability of silver nanoparticles to anchor to the bacterial cell wall and then penetrate it [53], (ii) the formation of free radicals by the silver nanoparticles which can damage the cell membrane and make it porous [54],(iii) releasing the silver ions by the nanoparticles, which can interact with the thiol groups of many vital enzymes and inactivate them [55, 56], and (iv) the nanoparticles can modulate the signal transduction in bacteria which stops the growth of bacteria [57], In this study silver sol with pure, SDS(A), Brij-58 (B) and mixed SDS+Brij-58 (C) surfactants system was tested for antibacterial activity against *Pseudomonas aeruginosa, Klebsiella Pneumonia and Micrococcus luteus* (Fig. 5).
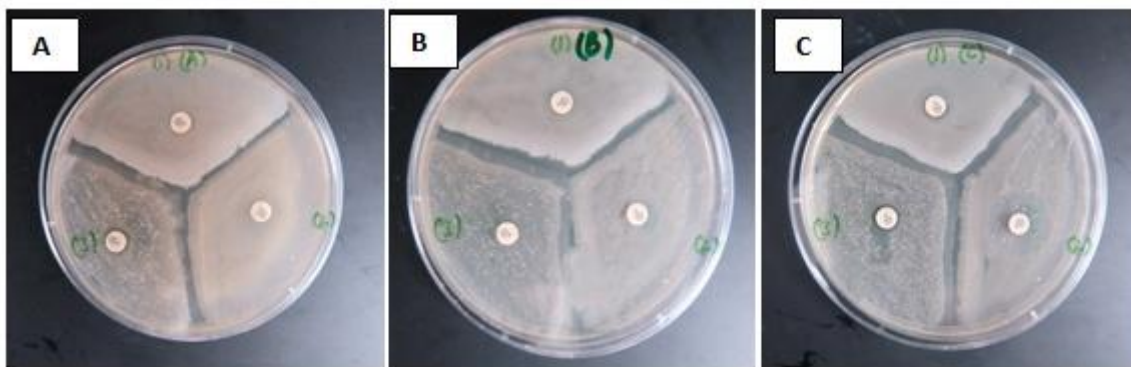
Figure 5. Disc diffusion method for antibacterial activity; (1) *P. aeruginosa*, (2) *Klebsiella Pneumonia* (3) *Micrococcus luteus*.

The mixed system (C) shows highest activity against both gram positive and negative bacteria (Fig. 5), but the silver sol with pure surfactants (A, B) did not show that much activity against these bacterial strains. A silver sol with mixed surfactant system exhibits outstanding antibacterial properties that could lead to biomedical applications.

4. CONCLUSIONS

1. For the present mixed systems, the *cmc* values are come out to be lower than *cmc*$_{ideal}$ values, suggesting synergism, also indicate non-ideal behavior of mixing.
2. The X_1^{ideal} values are lower than that of X_1, confirms a larger contribution of the SDS component to the mixed micelles than the ideal one and positive interaction in the mixed micellar phase.
3. The β^m values are not constant and –ve throughout, suggest the strong synergism in the system.
4. The A_{min} values for mixtures are higher than that of pure surfactants, suggests additional compactness of mixtures at the air/water interface, which could attribute to the orientation of the molecules at the interface.
5. Higher value of X^{σ}_1 compare to α_1 at lower mole fractions indicated more propensity of SDS to preferentially occupy the surface correlated to the Brij-58.
6. The values ΔH^m ΔG^m and ΔG^m_{ideal} are negative, but ΔS^m are positive, implying the spontaneous process of micellization.
7. The N_{agg} increases with the mole fraction of SDS. This can be explained on the basis of polydisperse nature of SDS, which could produce well-defined micelles of higher N_{agg}. This result is in line with previous results that mixed micelle contain more SDS (higher value of X_1).
8. High K_{sv} values suggest an increase in quenching due to the presence of both pyrene and quencher in the strong hydrophobic environment.
9. The values micropolarities (I_1/I_3) show alcohol like environment.
10. The present mixed system shows highest activity against both gram positive and negative bacteria, but the silver sol with pure surfactants did not show that much activity against these bacterial strains.

References

1. M.J. Rosen, *Surfactants and interfacial phenomena*, Wiley, New York (2004).
2. D. Myers, *Surfactant science and technology*, Wiley, New Jersey (2006).
3. T.F. Tadros, *Applied surfactants: principles and applications*, Wiley-VCH Verlag GmbH, Wenham (2005).
4. J.F. Scamehorn, *Phenomena in mixed surfactant systems*, ACS Symposium Series 311, American Chemical Society, Washington DC (1989).
5. M. Abe, K. Ogino, *Mixed surfactant systems*, Marcel Dekker, New York (1993).
6. E. Junquera, L. Pena, E. Aicart, *Langmuir,* 13 (1997) 219.
7. Q. Zhou, M.J. Rosen, *Langmuir,* 19 (2003) 4555.
8. N. Azum, M.A. Rub, A.M. Asiri, *Journal of Molecular Liquids*, 216 (2016) 94.
9. M.A. Rub, N. Azum, S.B. Khan, F. Khan, A.M. Asiri, *J Disp. Sci. Tech.*, 36 (2015) 521.
10. M.A. Rub, N. Azum, D. Kumar, F. Khan, A.M. Asiri, *J. Ind. Eng. Chem.*, 21(2015) 1119.
11. F. Khan, M.A. Rub, N. Azum, D. Kumar, A.M. Asiri, *J. Solution Chem.*, 44 (2015) 1937.
12. M.A. Rub, N. Azum, F. Khan, A.G. Al-Sehemi, A.M. Asiri, *Korean J. Chem. Eng.,* 32 (2015) 2142.
13. M.A. Rub, D. Kumar, N. Azum, F. Khan, A.M. Asiri, *Journal of Solution Chem.,* 43 (2014) 930.
14. N. Azum, M.A. Rub, A.M. Asiri, H.M. Marwani, *Journal of Molecular Liquids.*, 197 (2014) 339.
15. M.A. Rub, A.M. Asiri, N. Azum, Kabir-ud-Din, *J. Ind. Eng. Chem.*, 20 (2014) 2023.
16. N. Azum, M.A. Rub, A.M. Asiri, *Colloids and surfaces. B, Bioin.,* 121 (2014) 158.
17. N. Azum, M.A. Rub, A.M. Asiri, *Pharm. Chem. J.*, 48 (2014) 201.
18. M.A. Rub, N. Azum, D. Kumar, A.M. Asiri, H.M. Marwani, *Journal of Chemical Thermodynamics,* 74 (2014) 91.
19. N. Azum, M.A. Rub, A.M. Asiri, A.A.P. Khan, A. Khan, S.B. Khan, M.M. Rahman, A.O. Al-Youbi, *J. Solution Chem.*, 42 (2013) 1532.
20. A.A. Dar, G.M. Rather, A.R. Das, *J. Phys. Chem. B.*, 111 (2007) 3122.
21. T. Chakraborty, S. Ghosh, S.P. Moulik, *J. Phys. Chem. B.*, 109 (2005) 14813.
22. J.H. Clint, *Surfactant aggregation,* Chapman and Hall, New York (1992).
23. D.N. Rubingh, *Solution chemistry of surfactants,* Plenum, New York (1979).
24. K. Motomura, M. Aratono, In, *Mixed surfactant systems*, Dekker, New York (1998).
25. H. Maeda, *J. Colloid Interface Sci.*, 172 (1995) 98.
26. D.V. Talapin, E.V. Shevchenko, H. Weller, *Nanoparticles*. Wiley-VCH, Germany (2004).
27. C. Petit, S. Rusponi, H. Brune, *J. Appl. Phys.*, 95 (2004) 4251.
28. I.W. Park, M. Yoon, Y.M. Kim, Y. Kim, J.H. Kim, S. Kim, V. Volkov, *J. Magn. Magn. Mater.*, 272 (2004) 1413.
29. O. Masala, R. Seshadri, *Annu. Rev. Mater. Res.*, 34 (2004) 41.
30. R.C Baetzold, *J. Solid State Chem.*, 6 (1973) 352.
31. V. Sambhy, M. MacBride, B.R. Peterson, A. Sen, *J. Am. Chem. Soc.*, 128 (2006) 9798.
32. M.R. Elahifard, S. Rahimnejad, S., Haghighi, M.R. Gholami, *J. Am. Chem. Soc.*, 129 (2007) 9552.
33. D.M. Sturmer, A.P. Marchetti, J. Sturge, V. Waworth, A. Shepp, *Imaging Processes and Materials.* Wiley, New York (1989).
34. L. Jeunieau, V. Alin, J.B. Nagy, *Langmuir*, 16 (2000) 597.
35. M.J. Rosen, Q. Zhou. *Langmuir*, 17 (2001) 3532.

36. K. Tsubone, K.Y. Arakawa, M.J. Rosen, *J. Colloid Interface Science*, 262 (2003) 516.
37. M.J. Rosen, S. Aronson, *Colloid Surf.*, 3 (1981) 201.
38. M.A. Rub, F. Khan, M.S. Sheikh, N. Azum, A.M. Asiri, *J. Chem. Thermodynamics*, (2016), doi:10.1016/j.jct.2016.01.001
39. N. Azum, M.A. Rub, A.M. Asiri, M. Akram, *Russ. J. Phys. Chem. B*, 9 (2015) 940.
40. M.A. Rub, F. Khan, N. Azum, A.M. Asiri, Hadi M. Marwani, *J. Taiwan Inst. of Chem. Engs.* (2015), doi:10.1016/j.jtice.2015.10.017.
41. N.J. Turro, A. Yekta, *J. Am. Chem. Soc.*, 100 (1978) 5951.
42. K.K. Rohatgi-Mukherjee, *Fundamentals of Photochemistry*, Wiley Eastern, New Delhi (1992).
43. K. Kalyanasundram, J.K. Thomas, *J. Am. Chem. Soc.*, 99 (1977) 2039.
44. N. Azum, A.M. Asiri, M.A. Rub, A.A.P. Khan, A. Khan, M.M. Rahman, D. Kumar, A.O. Al-Youbi, *Colloid Journal.*, 75 (2013) 263.
45. N. Azum, M.A. Rub, A.M. Asiri, K.A. Alamry, H.M. Marwani, *J. Disp. Sci. Tech.*, 35 (2014) 358.
46. N. Azum, M.A. Rub, A.M. Asiri, *J. Molecular Liquids.*, 196 (2014) 14.
47. M.K. Al-Muhanna, M.A. Rub, N. Azum, S.B. Khan, A.M. Asir, *J. Chem. Thermodynamics.*, 89 (2015) 112.
48. N. Azum, M.A. Rub, A.M. Asiri, *J Disp. Sci. Tech.*, (2016), 10.1080/01932691.2016.1144197
49. R.C. Weast, *Handbook of Chemistry and Physics*, Palm Beach, CRC Press, FL (1978).
50. N.J. Turro, P.L. Kuo, P. Somasundaran, K. Wong, *J. Phys. Chem. B.,* 90 (1986) 288.
51. S.H. Kim, H.S. Lee, D.S. Ryu, S.J. Choi, D.S. Lee, *Korean J. Microbiol. Biotechnol.,* 39 (2011) 77.
52. S. Prabhu, E.K. Poulose, *Int. Nano Lett.*, 2 (2012) 1.
53. I. Sondi, B. Salopek-Sondi, *J. Colloid Interface Sci.*, 275 (2004) 177.
54. M. Danilcauk, A. Lund, J. Saldo, H. Yamada, J. Michalik, *Spectrochim. Acta, Part A.*, 63 (2006) 189.
55. Q.L. Feng, J. Wu, G.Q. Chen, F.Z. Cui, T.N. Kim, J.O. Kim, *J. Biomed. Mater. Res.*, 52 (2008) 662.
56. Y. Matsumura, K. Yoshikata, S. Kunisaki, T. Tsuchido, *Appl. Environ. Microbiol.,* 69 (2003) 4278.
57. S. Shrivastava, T. Bera, A. Roy, G. Singh, P. Ramachandrarao, D. Dash, *Nanotechnology.*, 18 (2007) 1.